Journal of Applied Fluid Mechanics, Vol. 12, No. 5, pp. 1475-1486, 2019.
Available online at www.jafmonline.net, ISSN 1735-3572, EISSN 1735-3645.
DOI: 10.29252/jafm.12.05.29770

A Numerical Study of the Frontal System between the Inflow and Outflow Waters in the Persian Gulf

A. Rahnemania[1], A. A. Bidokhti[2,†], M. Ezam[1], K. Lari[3] and S. Ghader[2]

[1] *Faculty of Natural Resources and Environment, Science and Research Branch, Islamic Azad University, Tehran 1477893855, Iran*
[2] *Institute of Geophysics, University of Tehran, Tehran 1417614418, Iran*
[3] *Department of Physical Oceanography, Faculty of Marine Science and Technology, Islamic Azad University, North Tehran Branch, Tehran 1987973133, Iran*

†*Corresponding Author email: Bidokhti@ut.ac.ir*

(Received October 21, 2018; accepted December 16, 2018)

ABSTRACT

In this study the dynamical characteristics of the salinity front between the Persian Gulf inflow and outflow were studied using the HYCOM numerical model. This model was integrated for 5 years from the beginning of 2011 to the end of 2015and the results of 2015 were discussed. The results of the model clearly showed seasonal variations in the salinity front in which the intrusion of the salinity front extends much farther into the Persian Gulf in summer. The salinity front appears to be prone to baroclinic instability with maximum intensity in spring and summer months (with a strong density stratification), forming cyclonic eddies (saline center) and anticyclones (sweeter center), that peaks in August. Results showed that some anti-cascade processes occur in mesoscale eddy activity, in agreement with the quasi-two-dimensional turbulence behavior. Spectral analysis of salinity time series in the front showed eddies with time scales ranging from a few hours to about 3 months. The result also showed that there was a reasonable relation between mixed layer depth and the formation of mesoscale eddies, so that mesoscale eddies disappeared when the thickness of mixed layer was increased in winter.

Keywords: Frontal system; Baroclinic instability; Mesoscale eddy; HYCOM; Persian Gulf.

1. INTRODUCTION

The Persian Gulf (PG) is a shallow water semi-enclosed basin in the south of Iran. It is bounded by desert area in the south and mountain ranges in the north. It is also sallower in the south than that of its northern region. Its average depth is about 35 m with maximum depth near the Strait Hormuz of about 110 m. After the Strait of Hormuz the depth water increases substantially to depths more than 2 km in the Oman Sea. PG is an evaporative basin with high salinity making it prone to thermhaline circulation through the Strait of Hormuz, as an inverse estuary, with no substantial sill.

The horizontal density gradient in the PG is mainly due to salinity gradient rather than temperature gradient. The PG has a 416 km^3/year water deficit, due to excessive evaporation and much less precipitation (Thoppil and Hogan, 2009, 2009). The water deficit is compensated for by the inflow of Oman Sea surface water through the Strait of Hormuz; denser and more saline waters exiting the PG near the bottom (Emery, 1956; Privett, 1959; Bower *et al.*, 2000; Bidokhti and Ezam, 2008; Yao, 2008). There also exist a seasonal surface outflow of intermediate salinity in the southern side of the Strait of Hormuz (Johns *et al.*, 2003). The dominant northwesterly winds called Shamal. in winter (November–February), mainly drive the surface water in the PG. These winds are stronger (5 m/s) in winter than those during the summer, June–September, (3 m/s). Hence, circulation in the Persian Gulf is mainly driven by these persistent northwesterly winds. These winds are cold in winter causing substantial surface cooling and hence convection in water column that erodes the seasonal thermocline in the PG in winter.

Between the Persian Gulf saline waters and the entering . fresher water from the Oman Sea, a salinity front forms in the Persian Gulf which change seasonally. This front is mainly buoyancy driven as opposed to some oceanic fronts generated by atmospheric forcing as those found for example in the Black Sea (Kazmin, 2016). Frontal systems due to

density difference can often produce some mesoscale eddies as those found in the yellow sea (Zhou *et al*., 2015). This front shows changes in relation to the impacts of different seasons and different weather conditions of the region. The research question is whether eddies formed along this salinity front, seen by observations, are due to instability along the salinity front? This instability can be baroclinic or barotropic, or even Kelvin Helmholtz. This instability appears intense in some seasons and seems to be initiated by the potential energy release, generating mesoscale eddies. Eddies play an important role in the transfer of energy, momentum, oxygen, transport of contaminations and algae blooms and nutrients, as well as mixing in the seas and oceanic environments. Apart from the scientific significance of this study, a better understanding of the eddy properties can contribute to the prediction of contamination of oil spills and other contaminants in the marine ecosystems of the PG. Previous studies have often focused on general circulation in the Persian Gulf. The mention of instability mechanisms in the Persian Gulf can be found in the Toppil and Hogan (2010), but issues such as turbulent spectra of such quasi-two-dimensional turbulence resulting from the some large scale instability, have not been investigated. In this research the HYCOM model that can adapt various vertical coordinate systems and is suitable for this study as the physical characteristics of this semi-enclosed seas can seasonally vary greatly, is used (Yao and Johns, 2010)

Features of the numerical model are described in the next section. The model set-up and the data used, are described in §3. The results of the model simulations are presented in §4. Time series and power spectral density of the flow in the front are discussed in §5. A summary of our results and conclusion is given in §6.

2. The Numerical Model And Its Configuration

The HYCOM ocean model used in this research has all three z-level, sigma, and isopycnal coordinate systems and can be used in shallow seas as well as in the deep ocean. The theoretical foundation for using such a coordinate was set by (Bleck and Boudra, 1981; Bleck and Benjamin, 1993). In HYCOM, each coordinate surface is assigned a reference isopycnal. The model continually checks whether or not grid points lie on their reference isopycnals and, if not, tries to move them vertically toward the latter. However, the grid points are not allowed to migrate when this would lead to excessive crowding of coordinate surfaces. Thus, in shallow water, vertical grid points are geometrically constrained to remain at a fixed depth while being allowed to join and follow their reference isopycnals over the adjacent deep ocean. In the mixed layer, grid points are placed vertically so that a smooth transition of each layer interface from an isopycnal to a constant-depth surface occurs where the interface outcrops into the mixed layer. HYCOM, therefore, operates as a conventional sigma model in very shallow and/or non-stratified oceanic regions, like a z-level coordinate model in the mixed layer or other non-stratified regions, and like an isopycnal-coordinate model in stratified regions. The model combines the advantages of the different types of coordinates in optimally simulating coastal and open-ocean circulation features. The present procedure of driving high-resolution coastal models (which invariably use fixed vertical grids) with the output from a basin-scale, isopycnal model can be streamlined since HYCOM will be able to provide the required near-shore data at fixed depth intervals (https://hycom.org).

HYCOM uses Arakawa C grid with momentum components, u, v carried at grid points and thermodynamics variables stored at pressure grid points. HYCOM is a finite-difference hydrostatic, Boussinesq Navier–Stokes (primitive equations) model that contains 5 prognostic equations: two for each horizontal velocity components, a layer thickness tendency (continuity equation), and two conservation equations for the pair of thermodynamic variables (salt, temperature or density) that is applied to a thin layer of stratified ocean on a rotating Earth (Bleck, 2002).

In HYCOM the ocean is vertically discretized as a set of stacked layers and the governing equations for each layer are given by integration over the layer. Within each layer, the temperature, salinity and the horizontal velocity components are determined and the pressure and fluxes, such as mass flux, momentum flux, heat flux and salt flux, are defined on the layers interfaces.

The solution in HYCOM model follows a program that is essentially working as a one-dimensional Arbitrary-Lagrangian-Eulerian (ALE) method. The ALE method uses a combination of Lagrangian and Eulerian reference frames and consists of two phases. Prognostic equations are combined with the explicit method of dividing of barotropic and baroclinic modes. The primary equations and operations in HYCOM are shown in (Fig. 1). The governing equations of HYCOM are formulated in a generalized coordinate framework where the vertical coordinate is automatically determined by the model through the water column conditions and can be either Cartesian z, pressure sigma σ or isopycnal, ρ. The model equations including momentum, continuity (as a layer thickness tendency equation) and themodynamic variables (temperature or salinity), written in (x, y, ξ) coordinates, where ξ is an one of the vertical coordinate, are (Bleck and Boudra, 1981; Bleck, 2002):

$$\frac{\partial \vec{V}}{\partial t} + \nabla_\xi \frac{\vec{V}^2}{2} + (\zeta + f)\hat{k} \times \vec{V} + \left(\dot{\xi}\frac{\partial p}{\partial \xi}\right)\frac{\partial \vec{V}}{\partial p} + \nabla_\xi M - p\nabla_\xi \alpha = -g\frac{\partial \vec{\tau}}{\partial p} + \left(\frac{\partial p}{\partial \xi}\right)^{-1}\nabla_\xi.\left(\upsilon\frac{\partial p}{\partial \xi}\nabla_\xi \vec{V}\right)$$

$$\frac{\partial}{\partial t}\left(\frac{\partial p}{\partial \xi}\right) + \nabla_\xi.\left(\vec{V}\frac{\partial p}{\partial \xi}\right) + \frac{\partial}{\partial \xi}\left(\dot{\xi}\frac{\partial p}{\partial \xi}\right) = 0$$

$$\frac{\partial}{\partial t}\left(\frac{\partial p}{\partial \xi}\theta\right) + \nabla_\xi.\left(\vec{V}\frac{\partial p}{\partial \xi}\theta\right) + \frac{\partial}{\partial \xi}\left(\dot{\xi}\frac{\partial p}{\partial \xi}\theta\right) = \nabla_\xi.\left(\upsilon\frac{\partial p}{\partial \xi}\nabla_\xi\theta\right) + \Pi_\theta \quad (1)$$

Where $\vec{V} = (u, v)$ represents the horizontal velocity vector, p is pressure, θ is any model's

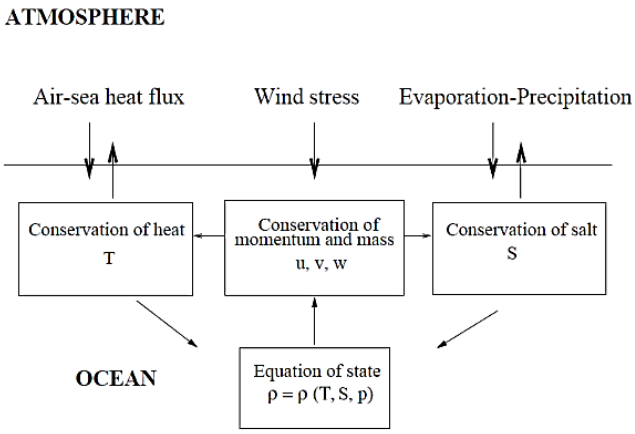

Fig. 1. A schematic diagram showing the conservation laws, prognostic variables and air-sea property fluxes used in HYCOM ocean model.

thermodynamic variables (temperature or salinity). $\alpha = \rho_\theta^{-1}$ is a potential specific volume, $\zeta = \frac{\partial v}{\partial x_\xi} - \frac{\partial u}{\partial y_\xi}$ is the relative vorticity, $M = gz + p\alpha$ is the Montgomery potential, $gz = \phi$ is the geopotential, f is the Coriolis parameter, $\hat{k}$ is the vertical unit vector, υ is the eddy viscosity/diffusion coefficient, $\vec{\tau}$ is the wind/bottom drag induced shear stress vector and Π_θ is the sum of diabatic source terms including diapycnal mixing acting on θ fields. Subscripts indicate which variable is held constant during partial differentiation and $\dot{\xi}$ shows time derivitive. For installing and configuring the model physics or architecture see (Wallcraft *et al*., 2003, 2009; Bleck *et al*., 2002; Bozec, 2013).

In this study the model domain is set between 22.46-30.55˚N and 47.5-59.9˚E that includes the entire Persian Gulf and most of the Oman Sea as indicated in Fig. 2. A Mercator grid projection is used and the horizontal resolution is set to 0.05 degree, which is thus capable of resolving mesoscale eddies realistically. There are 29 hybrid layers in the vertical where the deep minimum isopycnal spacing thickness is 1m and shallowest depth for isopycnal layers is 83 m. The top layer minimum thickness is 1 m and the density values (in sigma-T units) are from 16.75 to 27.82 kg/m^3. The baroclinic and barotropic time steps are 120 s and 15 s respectively. The bathymetry of the region was extracted from GEBCO (General Bathymetric Chart of the Oceans) which contains the global Earth topography including land with 30" resolution and was interpolated to the grid size of the model (https://www.gebco.net/data_and_products). A buffer zone is used at the eastern boundary in the Gulf of Oman where water properties are restored to monthly-observed values from WOA13 (World Ocean Atlas 2013). WOA13 is global gridded ocean temperature and salinity climatology data with a horizontal resolution of 0.25˚ and has 102 vertical levels (https://www.nodc.noaa.gov/OC5/woa13/woa13data.html).

The buffer zone has a width of about 50 km with an e-folding time scale of 1–78 days. The model integration was started from rest on January 1, 2011, using WOA13 temperature and salinity, and integrated for five years for the period 2011–2016 using 0.2˚, one-hourly NCEP-CFSV2 Meteorological forcing (https://www.climatedataguide.ucar.edu/climate-data/climate-forecast-system-reanalysis-cfsr). In particular, results from the year 2015 are used for detailed analysis of the mesoscale eddy activity. The simulations included the Mellor-Yamada level 2.5 turbulence closure scheme (Mellor and Yamada, 1982; Mellor, 1998). The interpolation and extrapolation were performed to map these data on to model grid in horizontal and vertical directions.

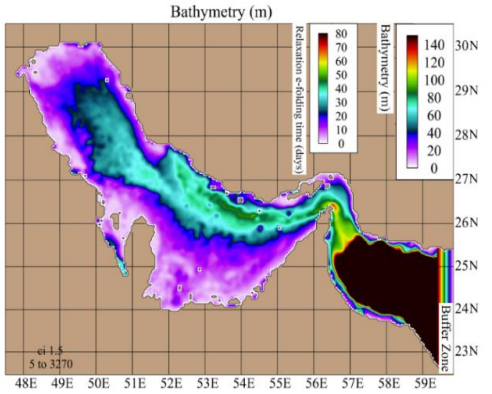

Fig. 2. Bathymetry of the Persian Gulf from GEBCO 30 second used for the model domain overlay with a Buffer zone.

3. RESULTS AND DISCUSSION

The model was integrated for 5 successive years (2011 to 2015) with 1 hourly varying forcing at the surface and lateral boundaries until a quasi-steady state was reached. The time series of basin averaged temperature and the domain-averaged surface salinity for the 5 years of integrations are shown in Fig. 3. Here, the results of the last year of the integration are presented.

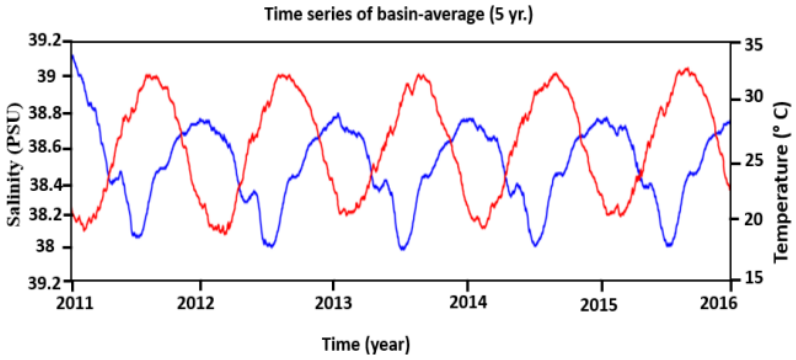

Fig. 3. Domain-averaged time series of sea surface salinity (blue) and temperature (red).

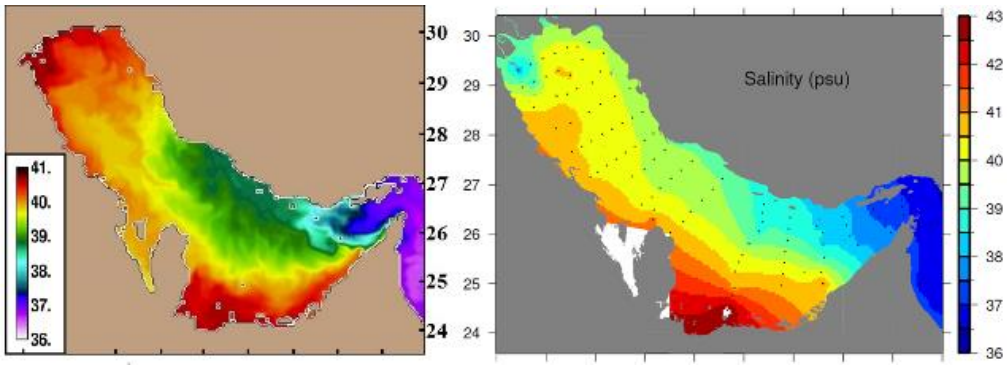

Fig. 4. Surface salinity field of ROPME observations [Yao *et al* 2010] (right) and results of model implementation (left) in early winter. River inflow was not considered in the simulations.

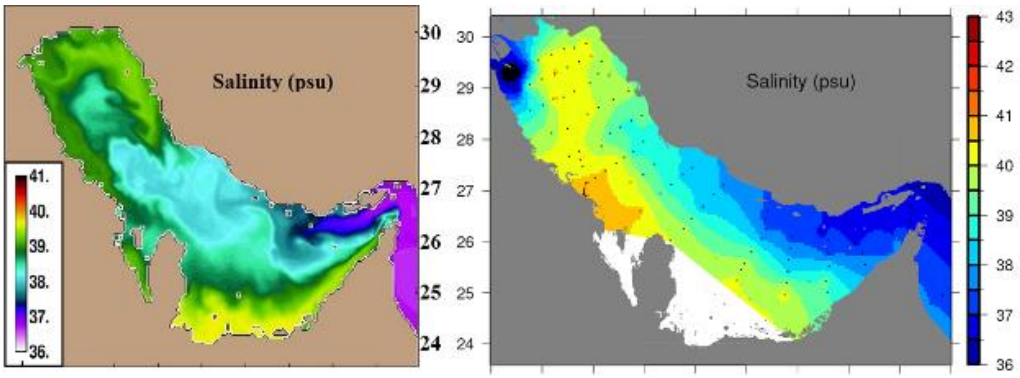

Fig. 5. Surface salinity field of ROPME observations [Yao *et al* 2010] (right) and results of model implementation (left) in early summer (without the river inflow in the model).

3.1 Comparison of Model Results with Observations

In this section, the results of model implementation are compared with some observations. Since field observations in the Persian Gulf have been sporadic and some of them are not reliable; only the comprehensive field measurements in the Persian Gulf obtained by ROPME project in 1992 are used. The data are measured at two different times by ROPME in 1992; which are for February 26 - March 11 (leg1) and May 20 to June 4 (leg 6). A good review of this data can be found in Reynolds (1993). Figures 4 and 5 compare the surface salinity fields of model simulations and observations. The salinity front in the Persian Gulf can reach up to 53° E in early summer, while it retreats to the Hormoz Strait (56 °E) in early winter and is generally in agreement with ROPME observations. However, the frontal structure and the associated eddies are pronounced in the simulations of salinity fields.

Figures 6 and 7 show the sea surface temperature of model simulations and ROPME observations for early summer and early winter. The results are generally consistent with the observations. The temperature field does not show frontal system as that of the seasonal variation of the field when is expressed by the salinity front. The salinity front is important in view of the fact that the boundary flows between the inflow and outflow waters are mainly controlled and marked by the salinity field and to some extent in temperature field of only model simulations.

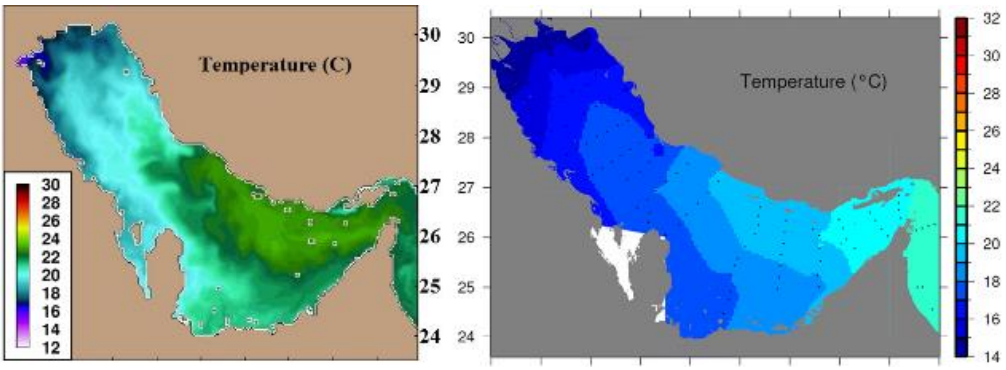

Fig. 6. Surface temperature field of ROPME observations [Yao *et al.*, 2010] (right) and results of model implementation (left) in early winter.

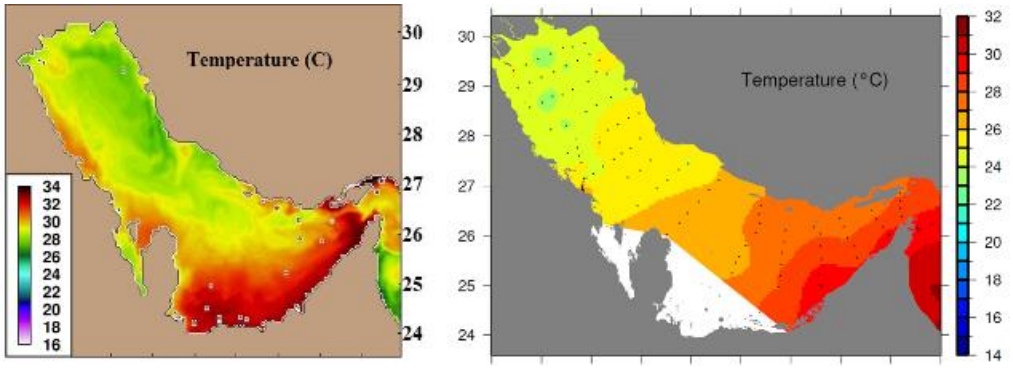

Fig. 7. Surface temperature field of ROPME observations [Yao *et al* 2010] (right) and results of model implementation (left) in early summer.

3.2 The Simulation Results of the Structure of the Salinity Front and Eddies

The Persian Gulf is an evaporation basin, so it has saltier water than that of the Oman Seawater hence, there is practically a salinity front between two water masses (Oman Sea and PG). The figure 8 shows the results of model at the surface based on the salinity field overlay with the current vector. The results indicate the changes in salinity front in each month of 2015. Based on the results, the salinity front is remarkably affected by seasonal changes as the intensity and position of front formation are changing over seasons. The location of front is steadily fluctuating between the Strait of Hormuz and the inner part of the PG. The most extended and retreat towards the Strait of Hormuz of the front (progression of front toward the PG) is recorded in winter and summer respectively. In January, the front retreats to 53°E near the Strait, which is maximum retreat. In the spring, the front has the maximum progression toward the inner part of the Persian Gulf up to 50°E in June. As it extends towards the inner part of the PG, it undergoes instability along the front in the basin (PG). As shown in Fig. 8, this instability is baroclinicy because of a strong horizontal density gradient between the water mass (Oman fresher water and PG salty water). In the summer the growth of instability creates mesoscale eddies. As theory predicts, when the slope of isopycnal enhances (in summer) instability of the front is more intense and more mesoscale eddies appear along the front and in winter the frontal instability is least (Fig. 8). In autumn, with the retreat of the salinity front, mesoscale eddies disappear to the extent that any size eddy can exist in the in this shallow sea.

Wind seems to influence the rate of extension of the front into the PG. Due to the northwesterly winds which have the highest speed in the winter, the front moves toward to the Oman Sea. Consequently, the saline front has the least extension in the PG. As the wind speed dramatically decreases in the spring the unstable front propagates into the PG.

Although we discuss the features of the front on the surface, the effect of the front is clearly observed near the bottom particularly in longitudinal transects of salinity and density fields (see Fig. 10).

3.3 The Structure of the Front

The slowly seasonal changes of the front are determined by the model simulations and some observations.

In a zone where the salinity front has seasonal variations, there are high salinity spatial gradients which also vary temporally. The horizontal gradient of salinity (hence density) according to the thermal equation ($\frac{\partial u}{\partial z} = \frac{1}{f}\frac{\partial \rho}{\partial y}$) is the main cause of the frontal instability, namely baroclinic instability. Because of the earth rotation the isopycnal lines are usually tilted in such frontal quasi-geostrophic system. Because in nature, in large-scale and mesoscale events, the

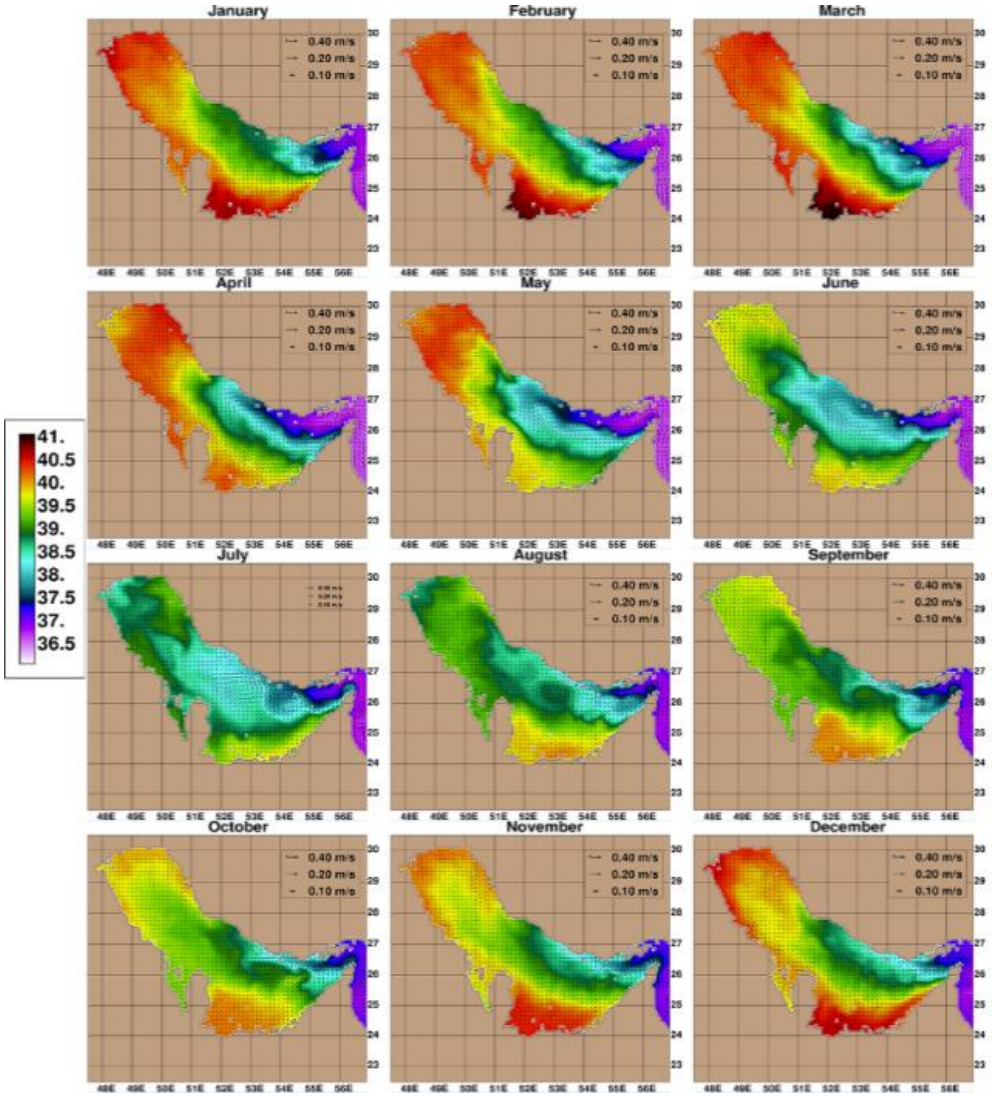

Fig. 8. Sea surface salinity fields overlaid with the current vectors in different months of 2015 (Last year's run).

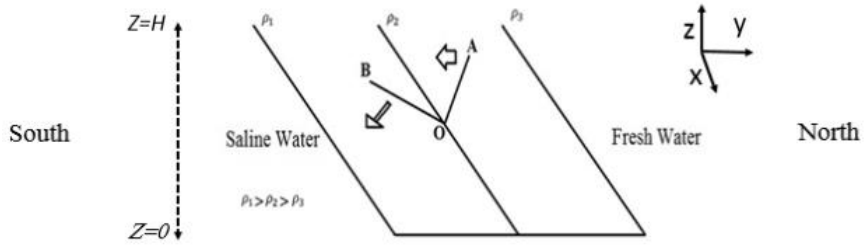

Fig. 9. Schematic formation of baroclinic instability in a density stratified ocean with the effect of earth rotation (see text for explanations).

Coriolis force does not allow the direct convection and it tilts the isopycnal lines (as in Fig. 9). The horizontal density gradient (two water masses of fresher water from Oman Sea to saline Persian Gulf water) leads tothe vertical gradient of horizontal velocity (two opposite directions of inflow and outflow) that causes baroclini c instability. Figure 9 shows baroclinic instability in a rotating system. Isopycnic lines tend to be tilt due to Coriolis force. In this form, the point A is stable relative to O, but B is unstable relative to O and the system becomes unstable when it is disturbed horizontally (exchanging A and B). Hence, the horizontal density gradient causes the baroclinic instability.

When vertical velocity gradient increases to a certain extent due to a horizontal density gradient which should be large enough, the large scale instability

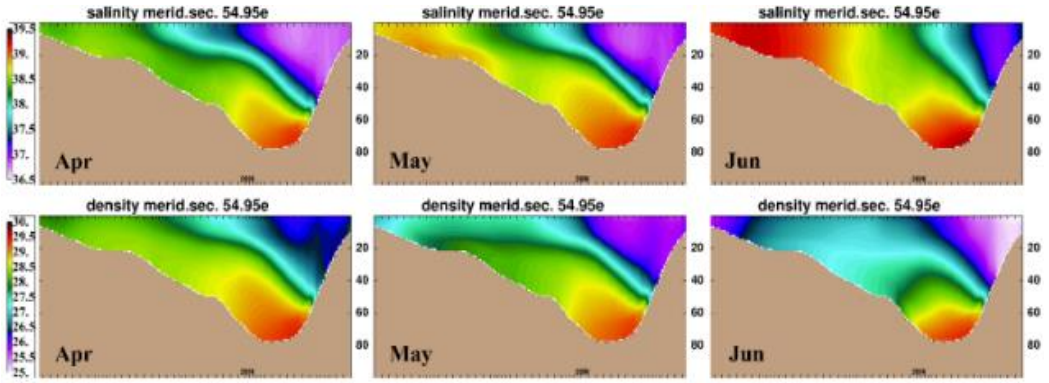

Fig. 10. Cross-section of salinity (upper) and density (lower) in the Persian Gulf near the Strait of Hormuz (54.95° E).

occurs. This is some kind of convection which is tilted because of the vertical component of convective flow is tilted (known as tilted convection, e.g. Vallis (2017). Figure 10 shows the cross-section of density and salinity near the Strait of Hormuz (54.95 °E) in the Persian Gulf, for the spring months indicating that baroclinic instability can occur and in that potential energy is converted into kinetic energy as in mesoscale eddies which enhances at the end of spring (compare Fig. 9 and Fig. 10).

As in Fig. 9, the governing equations for perturbation on the front can be given as:

$$\begin{aligned} &u_t + uu_x + vu_y - fv = -\rho_0^{-1} p_x \\ &v_t + uv_x + vv_y + fu = -\rho_0^{-1} p_y \\ &-p_z - \rho g = 0 \\ &u_x + v_y + w_z = 0 \\ &\rho_t + u\rho_x + v\rho_y + w\rho_z = 0 \end{aligned} \quad (2)$$

Where $\rho_0$is a constant reference density and indices represent partial derivatives. We assume that the flow consists of the main zonal speed $U(z)$, which is in the geostrophic balance with density $\overline{\rho}(y,z)$. Also (u, v, w) are the velocity components, ρ and p are the total density and pressure including changes due to perturbation, respectively. Using the two horizontal components of momentum equations, the vorticity equation can be obtained. By applying some mathematical operations, boundary conditions and also some assumptions (for details please see page 347 of Vallis (2017), the phase speed c of disturbance can be obtained by:

$$c = \frac{U_0}{2} \pm \frac{U_0}{\alpha H}\left[\left(\frac{\alpha H}{2} - tanh\frac{\alpha H}{2}\right)\left(\frac{\alpha H}{2} - coth\frac{\alpha H}{2}\right)\right]^{0.5} \quad (3)$$

$$\alpha = \frac{NH}{f}$$

Where t, U_0, and α are time, velocity at $z = H$ and Rossby radius of deformation respectively. N is buoyancy frequency which is calculated as $N = \left(\frac{-g}{\rho}\frac{\partial \rho}{\partial z}\right)^{0.5}$ and f is the Coriolis parameter and H is the depth of the front.

The critical condition for solution (stable and unstable) of the equation is obtained as follows:

$$\frac{\alpha_c H}{2} = \coth\left(\frac{\alpha_c H}{2}\right) \quad (4)$$

The index c refers to the critical value for Rossby radius of deformation. Hence the baroclinic instability condition for a wave with orbital wavelength λ is:

$$\lambda > 2.6a$$

Then the wavelength that has the highest growth is:

$$\lambda_{max} = 3.9\alpha \quad (5)$$

Typical value of N in winter and spring are estimated 0.0015 and 0.018 s^{-1} respectively. H the depth of the front is calculated as 60 m. Hence, the ratio of λ/α is about 1.8 in spring (and summer) and 7 in winter. The λ/α in April, is about 3.5 which is the closest value to the theoretically calculated value by Eq. (5). As figure 8 also shows the start of major frontal activity seems to begin in April. As the water is shallow, it is also expected that the bottom friction may be important in the dynamics of this baroclinic development.

3.4 Structure and Dynamics of Eddies

Mesoscale eddies are usually created by the baroclinic instability in the ocean and have a time scale of several weeks to several months. Here, eddies are considered that have a time scale of the order of a month, so that eddies will be easily visible from the monthly model simulations. These eddies have significance roles in the transport of contamination, nutrients, oxygen, phytoplankton and other biological and non-biological components, due to their long lifetime. In the Persian, Gulf eddies are mostly formed along the main salinity front and are both cyclonic and anti-cyclonic. Cyclonic eddies have saline water center and anti-cyclonic eddies have a fresher water center. Unlike in the major ocean currents as the Gulf Stream, where the temperature structure creates instabilities and eddies of warm centers (anticyclonic) and cold centers (cyclonic), in the Persian Gulf, salinity structure is the main cause of instability. The mesoscale eddies are in a quasi-geostrophic state in which the effects of Coriolis and buoyancy are important for the preservation and

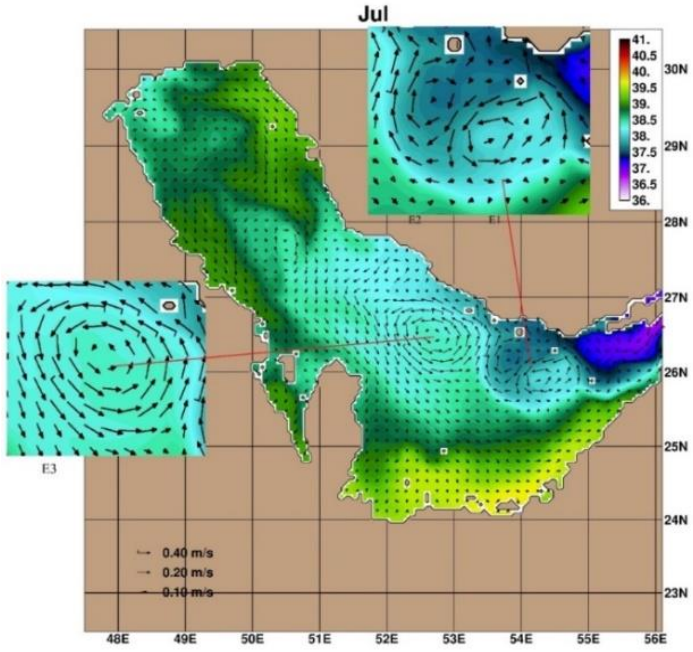

Fig. 11. Active eddies of the Persian Gulf in July from the 5th year of model simulations (2015).

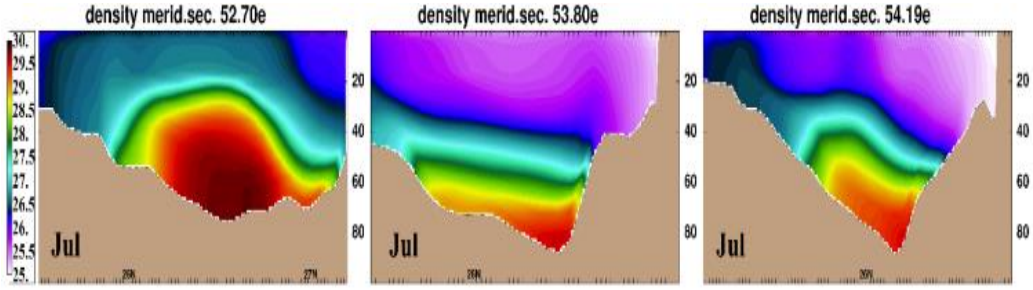

Fig. 12. Cross section of eddies in July in 2015 (E1 to E3 from right to left). See text for details.

sustainability of eddies which remain in the form of coherent structures. Also, the Coriolis causes eddies and inflow current to be to the right on the Iranian coast (Fig. 11). Another important factor in maintaining eddies is the vertical density stratification. Stratification limits the motion in a vertical direction and does not allow structures to decay in the form of three-dimensional turbulence in the vertical direction. A spectrum of eddies can be seen in the summer when the density stratification in the Persian Gulf is strong (when the seasonal thermocline is fully developed). In the boundary between two saline and fresher water masses, due to the large horizontal density gradient (Fig. 10), and hence, the vertical gradient of velocity (due to the opposite flows in both saline and fresher water masses of the front), instability leads to the formation of eddy structures. Verification of eddy structures requires high-resolution measurements. In this study, we will examine the mesoscale eddy structures which vary seasonally using numerical simulation results.

From July, the emergence of formed eddies begins as shown in Fig. 11. There are three main eddies in this month of which two are as a dipole of a cyclonic and anti-cyclonic twin with salty and fresher centers. These eddies are marked in Fig. 11 with E1, E2 are smaller and have an average radius of about 27 km. The larger eddy E3, which has a longer life time, has a radius of about 48 km. The latitude and longitude of these eddies in July are E1 (54.3° E, 25.9° N), E2 (53.8° E, 26.2 ° N), E3 (52.7° E, 26.5° N). Given the quasi-geostrophic nature of the eddy, we expect that the isopycnal lines are dome-shaped. So that in them pseudo-equilibrium to equilibrium conditions prevail. Figure 12 shows the cross-section of these eddies. Due to the importance of the structure of eddy, we discuss the different behavior of the eddy in different month separately.

August

In August, as in the summer strong stratification prevails and the salinity front spreads to the middle and northern parts of the Persian Gulf, it has the highest eddy activity (Fig. 13). There are 5 main eddies and E1 to E5, as indicated in the figure. As in July, cyclonic eddies have saline centers and anti-cyclonic eddies have fresher centers. Eddy E1 and E2 and E3 are eddies that have remained since July. But

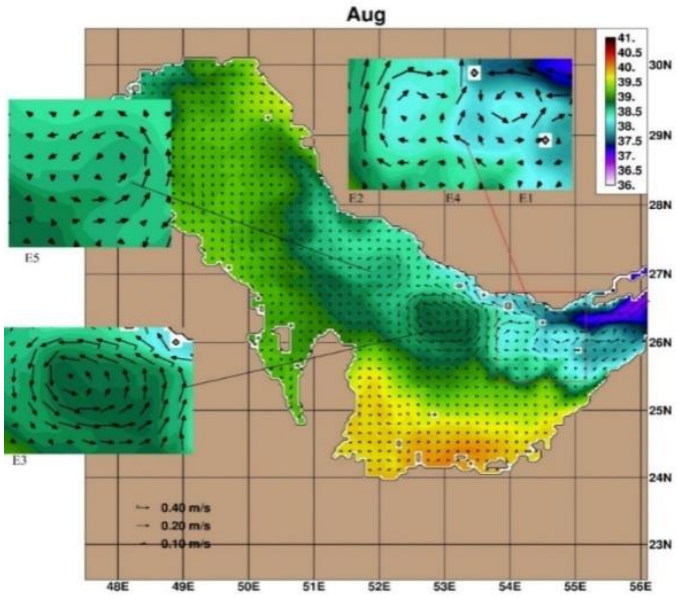

Fig. 13. Active eddies of Persian Gulf in August from the 5th year of model simulations (2015).

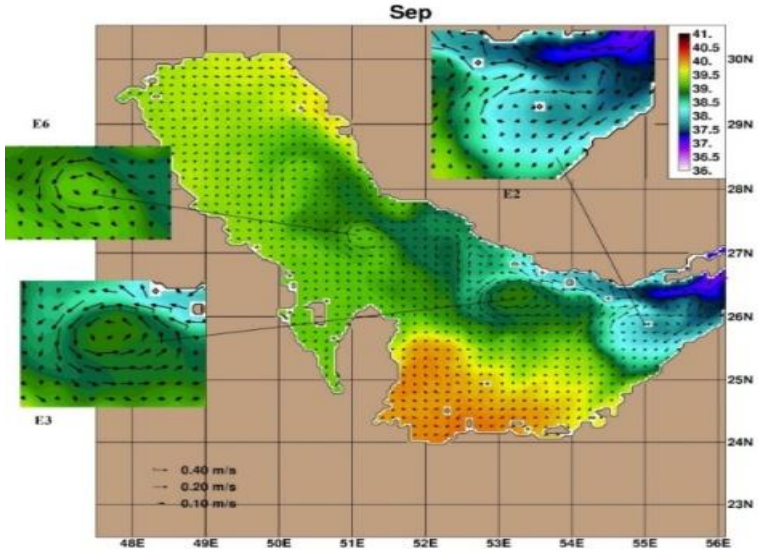

Fig. 14. Active eddies of the Persian Gulf in August from the 5thyear of model simulations (2015).

they have moved slightly east. The eddy E3 has a more saline center compared to that of July. The new eddy in August is a cyclonic eddy (E4), which is formed between the E1 and E2, and is probably created by the anti-cascade energy transfer processes (eddy merging, see below). Another new eddy in August is E5, as shown in the figure, due to the advance of the salinity front towards the northern part of the Persian Gulf and the ensuing instability in that area.

September

September is the end of the summer, due to the weakening of stratification and the retreat of the salinity front, it is expected that the structures of eddies will change as they fade away (Fig. 14). The most significant phenomenon that occurs during August-September seems to be the anti-cascade process. The anti-cascade process occurs only in two- and quasi two dimensional turbulence (Boffetta, 2012). In a three-dimensional turbulence, eddies can be converted to smaller eddies and on to the scale of Kolmogorov, and there is only a cascade of energy, while in the two-dimensional turbulence and as can be extracted from the enstrophy and energy spectra diagrams (e. g. Pedlosky, 2013), antic-cascade process is most likely to occur. Figure 15 shows the anti-cascade of energy processes during the period from August to September from which smaller eddies can merge to form larger eddies. The E3 eddy, which was in July and August, still exists in September but moved about 0.5 degrees (50 kilometers eastward). The E5 eddies disappeared in August, but new cyclonic eddies appeared at (51° E, 27 ° N) due to the retreat of the salinity front.

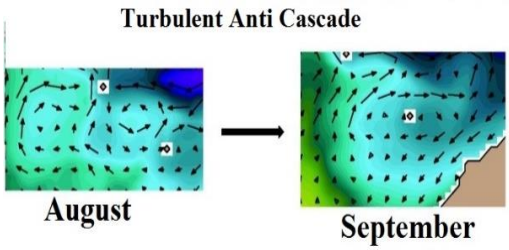

Fig. 15. Turbulent anti-cascade process in which two eddies merge to form a larger one from August to September.

3.5 Time Series and Power Spectrum Density in the Front

In this section, the time series their power spectral density of turbulence in the center of Persian Gulf (53 °E, 26° N), where the highest activity of eddies are due to progress of instability of the salinity front, are presented. Temperature and salinity time series are 6 hourly for the last year of the simulation (Figs. 16 and 17). Hence, harmonics (eddies) of frequencies less than $\frac{1}{6\,hr}$ can be analyzed. The time series of temperature is a pseudo-sinusoidal graph which is due to seasonal temperature variations in the Persian Gulf, and high-frequency fluctuations related daily variations and eddy and frontal activities. As expected, temperature fluctuations are less correlated with the eddy activity and instability, as temperature plays a minor role in eddy activity and frontal turbulence. Figure 17 show time series of salinity in the center of the Persian Gulf.

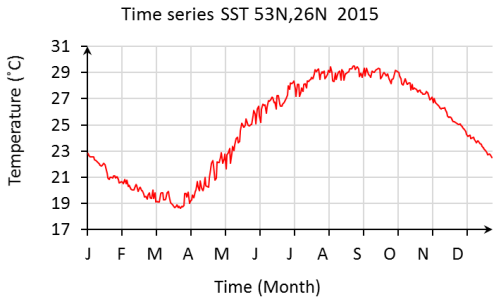

Fig. 16. Time series of Temperature in 53° E, 26° N for the 5thyear of model run (2015).

The very low frequency fluctuations are associated with the progress and retreat of the salinity front. Also, in spring and summer, a very low-frequency salinity drop is observed which is due to the progress of less saline water of the Oman Sea entering the PG. Fluctuations with rather lower frequencies are also observer which are mainly due to instability and mesoscale eddy activity (and possibly inertial-gravity wave activities) in spring and summer. The time series of salinity clearly illustrates the quasi two dimensional turbulent nature of the flow in this semi-enclosed sea. By providing the power spectral density of the salinity time series, one can obtain the type of turbulence and its spectrum. Figure 18 shows an example of power spectral density of salinity variations in terms of frequency, which indicates periods of about half day to several months for the turbulent eddies. Table 1 shows eddies having lifetimes longer more than a few days (extracted from Fig. 18). Also, the power spectral density gives a mean power of about f^{-2} for the turbulence spectrum, which indicates that turbulence has a spectrum similar to that of a two-dimensional turbulence (Vallis, 2017).

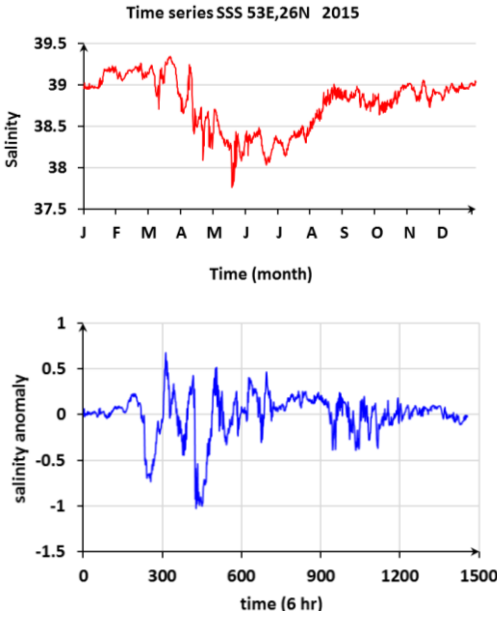

Fig. 17. Time series (6 hr int.) of surface salinity at 53° E, 26° N (above), anomaly series of salinity at 53° E, 26.5° N (below), from the 5thyear of model run (2015).

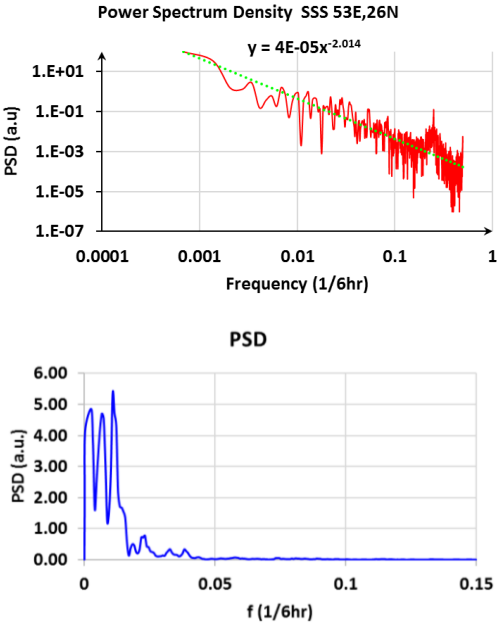

Fig. 18. Power Spectral density (PSD) of SSS in 53 °E, 26 ° N (above), PSD of anomaly of salinity at 53° E, 26.5° N (below), in last year of model run (2015).

It should be noted that eddies with life time of a few weeks to a few months are indicative of mesoscale eddies that are also common in open ocean. However, in this shallow sea they are expected to be more effected by bottom friction, a topics which we are about to investigate.

Table 1 Life time of eddies (days) calculated from the power spectral density in Fig. 18

frequency ($\frac{1}{6\ hr}$)	Life time of eddies (days)
0.0034	73.5
0.0055	45.5
0.007	35.7
0.01	25
0.013	19.2
0.015	16.7
0.02	12.5
0.027	9.3
0.034	7.4
0.039	6.4
0.04	6.3
0.046	5.4
0.05	5
0.0625	4

4. CONCLUSION

The dynamics of the boundary currents between inflow and outflow waters of the Persian Gulf using the HYCOM numerical model was investigated in this study. The model was executed using the initial condition of the WOA13 climatic data and the sponge boundary condition in the east boundary in the Oman Sea for 5 years from 2011 to 2015, and the results of 2015 were analyzed.

The results indicate that eddies formed along the salinity front, indicating that the salinity front is in a baroclinic instability state. Instability is sometimes very intense (March and April) indicating that the front is sharp and there is a lot of potential energy to be released in the sloping front. In some months as November and January as the whole water of the PG is mixed up, the retreated front has less potential energy for the release due to instability and more probably smaller scale instability may occur that needs higher resolution modeling. The Salinity front in December is in maximum retreat to the Strait and from January, the advancing of the salinity front begins and continues until late July, until it almost thread the whole length of the PG. The maximum advance of the salinity front is in July at which the formation of eddies are at its peak. Then it retreats from July and gradually continues until the late December, where the front reached near the Strait of Hormuz. This cycle of front behavior is associated with the sequential formation and destruction of seasonal thermocline in the Persian Gulf (Mosaddad *et al*., 2012).

Density stratification lasts from June to September, which coincides with the start and formation of eddies, and the loss of density stratification coincides with the fading of eddies since late September, meaning that density stratification is a major factor in the quasi-two-dimensional dynamics of the salinity front.

The mixed layer from April to September near the surface is gradually deepens from September to December. The deepest mixed layer is in December, which has gone down close to the bed. There is a direct relationship between the deepening of the mixed layer and the retreat of the salinity front. The anti-cascade process of large scale turbulence in the eddy spectrum inferred from the results of the model implementation is the property of two-dimensional turbulent and is in agreement with such spectrum of large scale flows in ocean and atmosphere. Eddies gradually move eastward over their lifetime. The Cyclonic eddies have saline centers, and the anti-cyclonic ones have a sweeter center. One of the dynamic characteristics of the frontier flow is that the intensity of the surface water entering the Persian Gulf is directly related to the intensity of the outlet water, so that when the deep outlet flow is weak, the surface inflow is also weakened, as well as if the deep outflow current is strong the inflow of the surface is also stronger, which can be attributed to the depletion of saline water from the Persian Gulf and the change in the pressure gradient between the Persian Gulf and the Oman Sea.

The tilted isopycnal surfaces also show the dynamic properties of the salinity front in the PG in which with the effect of Earth's rotation, it undergoes baroclinic instability which is strongest in spring and summer. Spectral analysis of salinity time series in the salinity front shows the eddies with varied time scales ranging from a few days to about 3 months The spectral characteristics is similar to that of large scale two-dimensional turbulence. Higher resolution simulations are required to investigate the smaller scale eddies such as sub-mesoscale eddies.

ACKNOWLEDGMENTS

The help of Dr. Alan Wallcraft and Dr. Alexandra Bozec of Florida State University in setting up the model is greatly acknowledged.

REFERENCES

Bidokhti, A. A. and M. Ezam (2008). The structure of the Persian Gulf outflow subjected to density variations. *Ocean Science Discussions 5* (2), 135-161.

Bleck, R. (2002). An oceanic general circulation model framed in hybrid isopycnic-Cartesian coordinates, *Ocean Model* 37, 55–88.

Bleck, R. and D. B. Boudra (1981). Initial testing of a numerical ocean circulation model using a hybrid (quasi-isopycnic) vertical coordinate. *Journal of Physical Oceanography 11* (6), 755-770.

Bleck, R. and S. G. Benjamin (1993). Regional weather prediction with a model combining

terrain-following and isentropic coordinates. Part I: Model description. *Monthly Weather Review 121* (6), 1770-1785.

Bleck, R., G. R. Halliwell, A. J. Wallcraft, S. Carroll, K. Kelly and K. Rushing (2002). Hybrid Coordinate Ocean Model (HYCOM) user's manual: Details of the numerical code. *HYCOM, version, 2* (01).

Boffetta, G. and R. E. Ecke (2012). Two-dimensional turbulence. *Annual Review of Fluid Mechanics 44*, 427-451.

Bower, A. S., H. D. Hunt and J. F. Price (2000). Character and dynamics of the Red Sea and Persian Gulf outflows. *Journal of Geophysical Research: Oceans 105* (C3), 6387-6414.

Bozec, A. (2013). *Hybrid Coordinate Ocean Model*, Hycom for Dummies.

Emery, K. O. (1956). Sediments and water of Persian Gulf. *AAPG Bulletin 40* (10), 2354-2383.

Johns, W. E., F. Yao, D. B. Olson, S. A. Josey, J. P. Grist and D. A. Smeed (2003). Observations of seasonal exchange through the Straits of Hormuz and the inferred heat and freshwater budgets of the Persian Gulf. *Journal of Geophysical Research: Oceans 108* (C12).

Kazmin, A. S. (2016). Persistent thermal fronts in the Black Sea: Existence, variability, and response to atmospheric forcing. *Oceanology 56* (3), 336-341.

Mellor, G. L. (1998). *Users guide for a three dimensional, primitive equation, numerical ocean model*. Princeton, NJ: Program in Atmospheric and Oceanic Sciences, Princeton University.

Mellor, G. L. and T. Yamada (1982). Development of a turbulence closure model for geophysical fluid problems. *Reviews of Geophysics 20* (4), 851-875.

Mosaddad, S. M., A. A. Bidokhti and H. Basirparsa (2012). An Observational and Numerical Modeling of Thermocline Development in the Persian Gulf. *Marine Geodesy 35* (1), 32-48.

Pedlosky, J. (2013). *Geophysical fluid dynamics*. Springer Science & Business Media.

Privett, D. W. (1959). Monthly charts of evaporation from the N. Indian Ocean (including the Red Sea and the Persian Gulf). *Quarterly Journal of the Royal Meteorological Society 85* (366), 424-428.

Reynolds, R. M. (1993). *Overview of physical oceanographic measurements taken during the Mt. Mitchell Cruise to the ROPME Sea Area* (No. BNL-49194; CONF-9301123-1). Brookhaven National Lab., Upton, NY (United States).

Thoppil, P. G. and P. J. Hogan (2009). On the mechanisms of episodic salinity outflow events in the Strait of Hormuz. *Journal of Physical Oceanography 39* (6), 1340-1360.

Thoppil, P. G. and P. J. Hogan (2010). A modeling study of circulation and eddies in the Persian Gulf. *Journal of Physical Oceanography 40* (9), 2122-2134.

Thoppil, P. G. and P. J. Hogan (2010). Persian Gulf response to a wintertime shamal wind event. *Deep Sea Research Part I: Oceanographic Research Papers 57*(8), 946-955.

Vallis, G. K. (2017). *Atmospheric and oceanic fluid dynamics*. Cambridge University Press.

Wallcraft, A. J., E. J. Metzger and S. N. Carroll (2009). *Software design description for the hybrid coordinate ocean model (HYCOM), Version 2.2* (No. NRL/MR/7320--09-9166). Naval Research Lab Stennis Space Center MS OCEANOGRAPHY DIV.

Wallcraft, A., S. N. Carroll, K. A. Kelly and K. V. Rushing (2003). *Hybrid Coordinate Ocean Model (HYCOM) Version 2.1. User's Guide*. Naval Research Lab Stennis Detachment Stennis Space Center MS.

Yao, F. (2008). Water mass formation and circulation in the Persian Gulf and water exchange with the Indian Ocean.

Yao, F. and W. E. Johns (2010). A HYCOM modeling study of the Persian Gulf: 1. Model configurations and surface circulation. *Journal of Geophysical Research: Oceans 115* (C11).

Yao, F. and W. E. Johns (2010). A HYCOM modeling study of the Persian Gulf: 2. Formation and export of Persian Gulf Water. *Journal of Geophysical Research: Oceans 115* (C11).

Zhou, C., P. Dong and G. Li (2015). A numerical study on the density driven circulation in the Yellow Sea Cold Water Mass. *Journal of Ocean University of China 14* (3), 457-463.